

Essential Role of Class II Phosphatidylinositol-3-kinase-C2 α in Sphingosine 1-Phosphate Receptor-1-mediated Signaling and Migration in Endothelial Cells^{*[5]}

Received for publication, August 14, 2012, and in revised form, November 20, 2012. Published, JBC Papers in Press, November 28, 2012, DOI 10.1074/jbc.M112.409656

Kuntal Biswas[‡], Kazuaki Yoshioka^{‡1}, Ken Asanuma[§], Yasuo Okamoto[‡], Noriko Takuwa^{‡¶}, Takehiko Sasaki[§], and Yoh Takuwa^{‡2}

From the [‡]Department of Physiology, Kanazawa University School of Medicine, 13-1 Takara-machi, Kanazawa, Ishikawa 920-8640, Japan, the [§]Department of Medical Biology, Graduate School of Medicine and Research Center for Biosignal, Akita University, Akita 010-8543, Japan, and the [¶]Department of Health and Medical Sciences, Ishikawa Prefectural Nursing University, Kahoku, Ishikawa 929-1210, Japan

Background: The role of phosphatidylinositol-3-kinase member PI3K-C2 α in actions of S1P is unknown, although it is implicated in membrane trafficking.

Results: PI3K-C2 α is essential for S1P-induced S1P₁ internalization, endosomal Rac1 activation, and cell migration in endothelial cells.

Conclusion: Internalized S1P₁ generates Rac signal and participates in cell migration.

Significance: PI3K-C2 α controls receptor-mediated cell signaling and migration by regulating vesicular trafficking.

The phosphatidylinositol (PtdIns) 3-kinase (PI3K) family regulates diverse cellular processes, including cell proliferation, migration, and vesicular trafficking, through catalyzing 3'-phosphorylation of phosphoinositides. In contrast to class I PI3Ks, including p110 α and p110 β , functional roles of class II PI3Ks, comprising PI3K-C2 α , PI3K-C2 β , and PI3K-C2 γ , are little understood. The lysophospholipid mediator sphingosine 1-phosphate (S1P) plays the important roles in regulating vascular functions, including vascular formation and barrier integrity, via the G-protein-coupled receptors S1P_{1–3}. We studied the roles of PI3K-C2 α in S1P-induced endothelial cell (EC) migration and tube formation. S1P stimulated cell migration and activation of Akt, ERK, and Rac1, the latter of which acts as a signaling molecule essential for cell migration and tube formation, via S1P₁ in ECs. Knockdown of either PI3K-C2 α or class I p110 β markedly inhibited S1P-induced migration, lamellipodium formation, and tube formation, whereas that of p110 α or Vps34 did not. Only p110 β was necessary for S1P-induced Akt activation, but both PI3K-C2 α and p110 β were required for Rac1 activation. FRET imaging showed that S1P induced Rac1 activation in both the plasma membrane and PtdIns 3-phosphate (PtdIns(3)P)-enriched endosomes. Knockdown of PI3K-C2 α but not p110 β markedly reduced PtdIns(3)P-enriched endosomes and suppressed endosomal Rac1 activation. Also, knockdown of PI3K-C2 α but not p110 β suppressed S1P-induced S1P₁ internalization into PtdIns(3)P-enriched endosomes. Finally, pharmacological inhibition of endocytosis suppressed S1P-in-

duced S1P₁ internalization, Rac1 activation, migration, and tube formation. These observations indicate that PI3K-C2 α plays the crucial role in S1P₁ internalization into the intracellular vesicular compartment, Rac1 activation on endosomes, and thereby migration through regulating vesicular trafficking in ECs.

Phosphatidylinositol (PtdIns)³ 3-kinases (PI3Ks), the family of enzymes responsible for the generation of 3'-phosphorylated phosphoinositides, have been extensively studied, and it is now established that PI3Ks are crucial components of many signaling pathways (1–3). Among the three classes of PI3K members, the majority of these studies have been focused on class I PI3Ks, and their main *in vivo* product is PtdIns 3,4,5-trisphosphates (PtdIns(3,4,5)P₃). Vps34, the sole member of class III, generates PtdIns 3-phosphate (PtdIns(3)P) to regulate vesicular trafficking/autophagy (4). Class II PI3Ks comprise three members, PI3K-C2 α (C2 α), PI3K-C2 β (C2 β), and PI3K-C2 γ , and mainly produce PtdIns(3)P *in vivo* (5–7). C2 α is distinct from the other members of PI3Ks due to its unique structure of the presence of a clathrin-binding domain in the N terminus (8). C2 α is enriched in clathrin-coated endocytic vesicles, endosomes, and the *trans*-Golgi network and has been implicated in the regulation of intracellular vesicular trafficking (9, 10). C2 α is expressed in a restricted pattern (*i.e.* mainly in the epithelium, vascular endothelium, and smooth muscle) (11, 12).

Recently, we showed that C2 α plays a crucial role in developmental and pathological angiogenesis and maintenance of the endothelial barrier function in an EC-autonomous manner

* This work was supported in part by grants-in-aid from the Japanese Ministry of Education, Culture, Sports, Science, and Technology; the Japan Society for the Promotion of Science; the Honjin Foundation; the Mitsubishi Pharma Research Foundation; and the SENSIN Medical Research Foundation.

[5] This article contains supplemental Movies 1–4.

¹ To whom correspondence may be addressed. Tel.: 81-76-265-2166; Fax: 81-76-234-4223; E-mail: yoshioka@med.kanazawa-u.ac.jp.

² To whom correspondence may be addressed. Tel.: 81-76-265-2165; Fax: 81-76-234-4223; E-mail: ytakuwa@med.kanazawa-u.ac.jp.

³ The abbreviations used are: PtdIns, phosphatidylinositol; S1P, sphingosine 1-phosphate; C2 α , PI3K-C2 α ; C2 β , PI3K-C2 β ; EC, endothelial cell; HUVEC, human umbilical vein endothelial cell(s); qPCR, quantitative real-time PCR; GEF, guanine nucleotide exchange factor; CFP, cyan fluorescent protein; sc-siRNA, scrambled siRNA; PH, pleckstrin homology.

through regulating vesicular trafficking (13). Global and endothelial cell (EC)-specific C2 α -null mice were embryonic lethal due to defects in angiogenesis. C2 α knockdown in ECs reduced PtdIns(3)P-enriched endosomes, impaired endosomal trafficking, and caused defective delivery of VE-cadherin to EC junctions and its assembly. C2 α knockdown also impeded cell signaling, including vascular endothelial growth factor receptor internalization and endosomal RhoA activation. These together led to defective EC migration, proliferation, tube formation, and barrier integrity. Endothelial PI3K-C2 α deletion suppressed postischemic and tumor angiogenesis and compromised vascular barrier integrity with augmented susceptibility to anaphylaxis and a higher incidence of dissecting aortic aneurysm formation (13).

Sphingosine 1-phosphate (S1P), a bioactive lysophospholipid mediator, induces diverse cellular responses, including cell migration, proliferation, survival, and differentiation, mainly through five S1P-specific G-protein-coupled receptors, S1P₁₋₅ (14–19). S1P₁, S1P₂, and S1P₃ are widely expressed in various tissues and are major receptors in the vasculature (18, 20). In vascular ECs, S1P stimulates cell migration and facilitates intercellular adherens junction formation mainly via S1P₁ and, to a lesser extent, S1P₃ (21–24). Targeted disruption of the S1P₁ gene in mice impairs vascular angiogenesis, maturation, or stabilization (25–27), indicating the significance of S1P-S1P₁ signaling axis in vascular formation.

Rho family GTPases have emerged as key regulators of cell migration and cell adhesion. Specifically, Rac activity is increased at the leading edge of migrating cells (28). This activity drives the formation of lamellipodial protrusion and subsequent forward movement of cells (29, 30). Rac activity also directs the formation of focal complexes (30–32). Cell motility critically relies on localized signaling. Recent studies suggested that Rac activation occurs on early endosomes, where a Rac-guanine nucleotide exchange factor (GEF) is also recruited (33–35). Further studies showed that controlled intracellular trafficking of Rac is important for spatially proper activation and actions of Rac (29, 35). Thus, the mechanism of endosomal Rac activation may be required for the spatial resolution of Rac-dependent mitogenic signals. Previous studies suggested that S1P₁-mediated activation of Rac plays a crucial role in S1P-directed migration of ECs (20, 22). However, it is unknown how S1P₁ regulates Rac activity spatially within cells.

In this study, we investigated the role of C2 α for S1P-induced EC migration and activation of cellular signaling. Our data demonstrate for the first time that C2 α is pivotal for S1P-induced cell migration, lamellipodium formation, and tube formation in ECs. Importantly, C2 α is also essential for the particular cell signaling, Rac1 activation; S1P-induced Rac1 activation occurs on endosomes, in which internalized S1P₁ is co-localized, in a C2 α -dependent manner. Thus, these observations indicate that, different from the classical role of receptor internalization as a mechanism for receptor desensitization or inactivation, internalized S1P₁ serves a role for signaling on endosomes and thereby migration and morphogenesis and that these S1P-induced processes are orchestrated by C2 α .

EXPERIMENTAL PROCEDURES

Reagents and Constructs—The following antibodies and reagents were used: anti-C2 α antibody (catalog no. 611047, BD Pharmingen); anti-C2 β antibody (P91720, BD Transduction); anti-p110 α antibody (catalog no. 4249, Cell Signaling Technology (CST)); anti-p110 β antibody (catalog no. 3011, CST); anti-Rac1 antibody (catalog no. 05-389, Upstate-Millipore); anti-RhoA antibody (clone 26C4, sc-418, Santa Cruz Biotechnology, Inc., Santa Cruz, CA); anti-active GTP-Rac1 antibody (catalog no. 26903, NewEast Biosciences); anti-phospho-paxillin antibody (Tyr-118) (catalog no. 2541, CST); anti- α -tubulin antibody (MS-581-P0, NeoMarker); anti-Vps34 antibody (catalog no. 3358, CST); anti-phospho-p42/p44 MAPK antibody (ERK1/2, Thr-202/Tyr-204, catalog no. 4370, CST), anti-total p42/p44 MAPK antibody (ERK1/2, catalog no. 9102, CST), anti-phospho-Akt antibody (Ser-473, catalog no. 4060, CST), anti-total Akt antibody (catalog no. 9272, CST), anti-GSK-3 β (catalog no. 5676, CST), anti-phospho-GSK-3 β (Ser-9) (catalog no. 5558, CST), all AlexaFluor-conjugated secondary antibodies and AlexaFluor594-phalloidin (Molecular Probes, Inc.), 4',6-diamidino-2-phenylindole (DAPI) (Invitrogen), dynasore hydrate (Sigma), S1P (catalog no. SL-140, Enzo Life Sciences), W146 (catalog no. 10009109, Cayman), and Akt1/2 inhibitor VIII (catalog no. 124018, Calbiochem). GFP-2xFYVE and mRFP-2xFYVE expression vectors were obtained from Dr. H. Stenmark (University of Oslo) and Dr. Y. Ohsumi (Tokyo Institute of Technology), respectively. The expression vector for Rac1-FRET probe, Raichu-Rac (pRaichu-Rac1), was obtained from Dr. M. Matsuda (Kyoto University). S1P₁-mRFP expression vectors were constructed by standard PCR methods.

Cell Culture, Short Interfering RNAs (siRNAs), and Transfection—Human umbilical vein endothelial cells (HUVEC) (Lonza) of passages 2–5 were grown in endothelial basal medium supplemented with 2% fetal bovine serum (FBS) and a growth factor supplement mixture (EBM2TM; Lonza catalog no. CC-3162) on type I collagen-coated dishes. The cells were transfected with 20 nM siRNA using Lipofectamine 2000 (Invitrogen) in Opti-MEM (Invitrogen) according to the manufacturer's instructions. After 4 h, the media were replaced with EBM2. The cells were cultured for a further 24–48 h before processing for analysis. The human C2 α siRNA target sequence was 5'-AAGTTGGCACTTACAAGAAT-3' (the first nucleotide of the target sequence is positioned in the nucleotide 2182 when "A" of the start codon ATG of the mRNA sequence is numbered as 1). The human Vps34 target sequence was 5'-AAACTCAACACTGGCTAATTA-3' (the first nucleotide is positioned in the nucleotide 1513). The human p110 α target sequence was 5'-GGACAACACTGTTTCATATAG-3' (D-003018-7, Dharmacon). The human C2 β target sequence was 5'-AAGCCGGAAGCTTCTGGGTTT-3' (the first nucleotide is positioned in the nucleotide 2889). The human p110 β target sequence was 5'-AATCCCTCTAAATATCAGACC-3' (the first nucleotide is positioned in the nucleotide 1328). As a control, a scrambled duplex oligonucleotide with a C/G content equivalent to the positive oligonucleotide was used. All siRNAs were designed and synthesized using the siRNA construction kit (Ambion) according to the manufacturer's instructions.

Efficacy of RNA interference was confirmed by Western blotting using specific antibodies. The cells were transfected with the expression vectors for GFP/mRFP-2xFYVE and mRFP-S1P₁ by Amaxa Nucleofector (Lonza) according to the manufacturer's instructions.

Transwell Migration Assay—Transwell cell migration across a type I collagen-coated polycarbonate filter with 8- μ m pores (Neuroprobe) was determined using a modified Boyden chamber (a 96-blind well chamber; Neuroprobe) as described previously (36, 37). The indicated concentrations of S1P in M199 medium (Invitrogen) containing 0.25% fatty acid-free bovine serum albumin (BSA) (Sigma-Aldrich) were loaded into the lower wells. The siRNA-transfected HUVEC (1×10^5 cells/well) resuspended in 0.25% BSA-containing M199 medium were placed in the upper wells and allowed to migrate toward the lower chamber at 37 °C in 5% CO₂ for 6 h. The cells attached on the filter were fixed with methanol and stained with a Diff-Quick staining kit (Baxter Scientific Products). The upper side of the filter was then scraped free of cells. The number of cells on the lower side of membranes was determined by measuring optical densities at 595 nm using a 96-well microplate reader model 3550 (Bio-Rad).

Pull-down Assay of Small G-protein Activity—The pull-down assays for GTP-bound Rac1 and RhoA were performed as described previously (36, 38–40). In brief, HUVEC were stimulated and lysed with the Rac/Rho extraction buffer (50 mM Tris-HCl (pH7.5), 500 mM NaCl, 10 mM MgCl₂, 1% Triton X-100, 0.5% sodium deoxycholate, 0.1% SDS, 10% glycerol, 1 mM Na₃VO₄, 10 mM NaF, 10 mM sodium β -glycerophosphate, and Complete protease inhibitor mixture (Roche Applied Science)). The lysates were sonicated and cleared by centrifugation, and the resultant supernatants were incubated for 60 min at 4 °C with glutathione-Sepharose 4B beads (GE Healthcare) coupled to either the CRIB domain of PAK1 for Rac1 or the Rho binding domain of rhotekin for RhoA. The beads were washed, and bound proteins were solubilized by the addition of 50 μ l of 2 \times Laemmli's SDS-PAGE loading buffer, followed by separation on 15% SDS-polyacrylamide gels and Western blotting using anti-Rac1 or anti-RhoA antibodies. The band densities of Rac1 and RhoA were determined by densitometry. The amounts of GTP-Rac1 and GTP-RhoA were corrected for those of total Rac1 and RhoA, respectively, and the normalized quantified data were expressed as multiples over the values of non-treated control cells.

Tube Formation Assay—siRNA-transfected HUVEC (2.5×10^4 cells) in M199 containing 1% FBS were seeded onto 200 μ l of growth factor-reduced Matrigel (BD Biosciences) in a 24-well plate in the absence or presence of S1P and dynasore and incubated for 6–12 h (41). Tube formation was quantified by measuring cumulative tube length in five random microscopic fields/well with ImageJ software (National Institutes of Health).

Immunostaining—HUVEC cultured on cover slides or glass-bottomed dishes were serum-starved in M199 medium including 0.5% BSA overnight or for 6 h and stimulated with S1P (41). The cells were fixed in prewarmed 4% paraformaldehyde in Dulbecco's phosphate-buffered saline (PBS) for 15 min and then permeabilized in 0.2% Triton X-100 in PBS for 15 min

when necessary. After blocking, the cells were incubated with primary antibodies overnight and then incubated for 1 h with goat AlexaFluor488- or AlexaFluor594-conjugated secondary antibodies. The cells were counterstained with DAPI (Molecular Probes) for 5 min and mounted on Fluoromount. The stained cells were observed using a confocal laser-scanning microscope (Zeiss Axiovert 200M with LSM5 Pascal) equipped with a $\times 63$ /numerical aperture 1.4 PlanApo oil immersion objective. For quantification of the amount of positive pixels, the positive area in stained images in each frame was calculated using ImageJ software. Adobe Photoshop was used to adjust image levels and process image overlays.

Actin Filament (F-actin) Staining—HUVEC were treated with either vehicle or S1P, fixed in 3.7% formaldehyde or 4% paraformaldehyde in PBS, and permeabilized in 0.2% Triton X-100 in PBS, followed by staining with AlexaFluor594-conjugated phalloidin for F-actin, as described previously (37). Total cellular perimeter and lamellipodial perimeter per cell were measured by using ImageJ software, and the lamellipodial index (lamellipodial perimeter length/total cell perimeter $\times 100$) was determined.

FRET Imaging—HUVEC were transfected with the Rac FRET probe expression vector pRaichu-Rac1 (42), using the Amaxa Nucleofector system according to the manufacturer's instructions. The chimeric FRET probe protein consists of N-terminal yellow fluorescent protein (YFP), the CRIB domain of PAK1, Rac1, and C-terminal cyan fluorescent protein (CFP). When Rac1 in the chimeric FRET probe protein is bound to GDP, fluorescence of 475 nm emanates from CFP with excitation at 433 nm. When Rac1 is bound to GTP, intramolecular binding of GTP-loaded Rac to the CRIB domain brings YFP into close proximity to CFP, which causes FRET and fluorescence of 527 nm from YFP. For confocal FRET imaging, cells were serum-starved in phenol red-free M199, including 0.25% BSA, for 6 h. Then, the cells were incubated in a fresh medium with the same compositions and observed/imaged on a heated stage (37 °C) (Thermo Plate, Tokai-Hit) in an atmosphere of 5% CO₂ and 95% air (2GF-MIXER, Okolab) on an inverted microscope (model IX70, Olympus)-based high resolution confocal laser microscope system (CSU system, Yokogawa) equipped with a UPLSAPO $\times 60$ /numerical aperture 1.35 oil objective, an electron-multiplying charge-coupled device digital camera (iXon, Andor), and a light engine (Lumencor, Inc.) configured with a CFP/YFP filter set (Di01-T442/514/647-13 $\times 15 \times 0.5$, Semrock). The acquisition and process were controlled by iQ software (Andor). Images were taken at every 10-s interval, and movies were prepared at a frequency of 5 frames/s. Pseudo-gray scale ratio images were generated from images from CFP and FRET channels using Andor iQ software.

Imaging of GFP- and RFP-tagged Proteins—HUVEC were transfected with the expression vectors for GFP/mRFP-2xFYVE and S1P₁-mRFP, using the Amaxa Nucleofector system (Lonza), plated on glass-bottomed dishes (catalog no. P35G-1.5–20-C, MatTek), and allowed to adhere for 16 h before imaging. The cells were serum-starved in M199 medium, including 0.5% BSA, for 6 h and stimulated with S1P. The cells were fixed in 4% paraformaldehyde for 15 min and

PI3K-C2 α and S1P₁ Signaling

observed with a high resolution confocal laser microscope system (CSU System, Yokogawa), as described above.

Quantitative Real-time PCR (qPCR)—Total RNAs were extracted using TRIzol reagent (Invitrogen). Total RNA (1 μ g) was reverse-transcribed using a QuantiTect Transcription Kit (Qiagen). Absolute qPCR (absolute copy number quantification using the standard curve for each gene) was performed using qPCR MasterMix plus for SYBR assay (Eurogentec, RT-SY2X-03+WOU) in the ABI7300 real-time PCR system (Applied Biosystems), as described previously (13). The primers employed were as follows: for S1P₁, S1P1-F (tgcgggaagggtatgttt) and S1P1-R (cgatggcgaggactgaac); for S1P₂, S1P2-F (gcctctctacccaagcatta) and S1P2-R (ttgagcggaccacgcagta); for S1P₃, S1P3-F (ggtgattgtgtgagcgtgtt) and S1P3-R (aggccatcaatgaggaaga); for S1P₄, S1P4-F (aagaccagccgcgtcta) and S1P4-R (ccaggcagaagaggatgt); for S1P₅, S1P5-F (ggaaatgcagccaaagg) and S1P5-R (ccattttcatcaccgagtt); and for β -actin, β -actin-F (tctacaatgagctgcgtgtg) and β -actin-R (atggctgggtgtgaag). We have validated that these primer pairs are highly specific for each target without cross-amplification. Absolute quantification determined the actual copy numbers of target genes by relating the C_t value to a standard curve. The levels of S1P receptor mRNAs were expressed as multiples of mRNA level of the reference gene, β -actin.

Western Blot Analysis—The cells were washed in PBS and lysed in cell lysis buffer (50 mM Tris-HCl (pH 7.4), 150 mM NaCl, 5 mM EDTA, 1% Triton X-100, 1 mM Na₃VO₄, 10 mM NaF, 10 mM sodium β -glycerophosphate, and Complete protease inhibitor mixture) by scraping, and cell lysates were centrifuged for 10 min at 16,000 $\times g$ at 4 $^{\circ}$ C, the resulting supernatants taken for Western blotting. Cell lysates were subjected to 8 or 15% SDS-PAGE, followed by electrotransfer to polyvinylidene difluoride membranes (Millipore). After transfer, the membranes were blocked in 5% BSA, 0.1% Tween 80 in Tris-buffered saline (10 mM Tris (pH 7.5) and 150 mM NaCl). Target proteins were detected with specific antibodies. After incubation with the appropriate alkaline phosphatase-conjugated secondary antibodies, protein bands were visualized by the color reaction using the nitro blue tetrazolium chloride/5-bromo-4-chloro-3'-indolylphosphatase *p*-toluidine system (Sigma).

Metabolic Cell Labeling, Lipid Extraction, and Phosphoinositide Measurements—The amounts of cellular phosphoinositides were determined as described (43, 44). In brief, HUVEC in 10-cm dishes were serum-starved in phosphate-free Dulbecco's minimal essential medium (DMEM) for 1 h and labeled by [³²P]orthophosphate (1 mCi/dish; PerkinElmer Life Sciences) for 4 h in phosphate-free DMEM. The labeled cells were stimulated as indicated. The cells were washed twice with ice-cold PBS and quickly scraped in 800 μ l of 2% HClO₄. Resulting extracts were mixed with 3 ml of chloroform/methanol (1:2) and vortexed. The mixture were then incubated at room temperature for 10 min and mixed with each 1 ml of CHCl₃ and 2% HClO₄ to separate the organic and aqueous phases. After centrifugation, the lower organic phase was recovered and mixed with 1 ml of CHCl₃-saturated 0.5% NaCl and 1% HClO₄. The mixture was vortexed well and then centrifuged. After centrifugation, the lower organic phase was recovered and dried in a vacuum centrifuge. Dried lipids were deacylated with 1 ml of

40% methylamine/H₂O/methanol/*n*-butanol (24:16:40:10), incubated at 53 $^{\circ}$ C for 1 h, dried in a vacuum centrifuge, and resuspended in 800 μ l of *n*-butanol/petroleum ether/ethyl formate (20:40:1) and 800 μ l of H₂O. After centrifugation, the aqueous phase was transferred and dried in a vacuum centrifuge. The resulting samples were resuspended in 130 μ l of 10 mM (NH₄)₂HPO₄ and analyzed by high performance liquid chromatography (HPLC) using a Partisphere SAX column (Whatman), as described (43, 44). The radioactivity of each fraction was determined by scintillation counting. The amounts of PtdIns(3)P and PtdIns(3,4,5)P₃ were expressed as the ratios of the radioactivities of PtdIns(3)P or PtdIns(3,4,5)P₃ over those of PtdIns(4)P plus PtdIns(4,5)P₂, as described previously (43, 44).

Statistical Analysis—All the data are presented as the means \pm S.E. and were analyzed using Prism 5 software (GraphPad Software Inc., San Diego, CA). All statistical analysis was performed either by one-way or two-way analysis of variance with a subsequent post hoc test. Results with $p < 0.05$ were considered statistically significant.

RESULTS

S1P₁-mediated Cell Migration of HUVEC Is Dependent on Class II PI3K-C2 α —The HUVEC expressed S1P₁ most abundantly and S1P₃ less prominently but did not detectably express S1P₂, S1P₄, or S1P₅, as determined by qPCR analysis (Fig. 1A). As reported previously (22–24), S1P stimulated transwell migration of HUVEC with increased phosphorylation of Akt, a protein kinase activated downstream of PI3K (Fig. 1, B and C). Because S1P₁ mediates cell migration through a PI3K-dependent mechanism (36, 45), we examined whether S1P-stimulated migration and Akt phosphorylation in HUVEC were mediated by S1P₁ or not. The S1P₁-selective antagonist W146 abolished S1P-induced cell migration (Fig. 1B) and Akt phosphorylation (Fig. 1C), indicating that both responses were mediated by S1P₁.

We studied the role of C2 α in S1P₁-mediated cell migration. The HUVEC were transfected with either of the specific siRNAs targeting class I p110 α and p110 β , class II C2 α and C2 β , and class III Vps34 or scrambled siRNA (sc-siRNA) duplex as a control. Each specific siRNA effectively inhibited the expression of respective PI3K proteins (Fig. 1D). Knockdown of p110 β or C2 α substantially inhibited S1P-directed cell migration, and that of C2 β , to a lesser extent, inhibited S1P-directed migration (Fig. 1E). Knockdown of p110 α or Vps34 showed no inhibitory effect. We previously showed in HUVEC that C2 α knockdown reduced GFP-FYVE-positive vesicles and inhibited their motility (13). In this study, we determined the effects of knockdown of C2 α and p110 β on the total cellular levels of PtdIns(3)P and PtdIns(3,4,5)P₃ in HUVEC by HPLC analysis of cellular lipids. C2 α knockdown did not affect the cellular contents of PtdIns(3)P or PtdIns(3,4,5)P₃ in non-treated HUVEC (Fig. 1F). S1P stimulation did not change the cellular levels of PtdIns(3)P or PtdIns(3,4,5)P₃. Knockdown of p110 β did not affect the cellular contents of PtdIns(3)P or PtdIns(3,4,5)P₃ in S1P-stimulated or non-stimulated HUVEC (Fig. 1G).

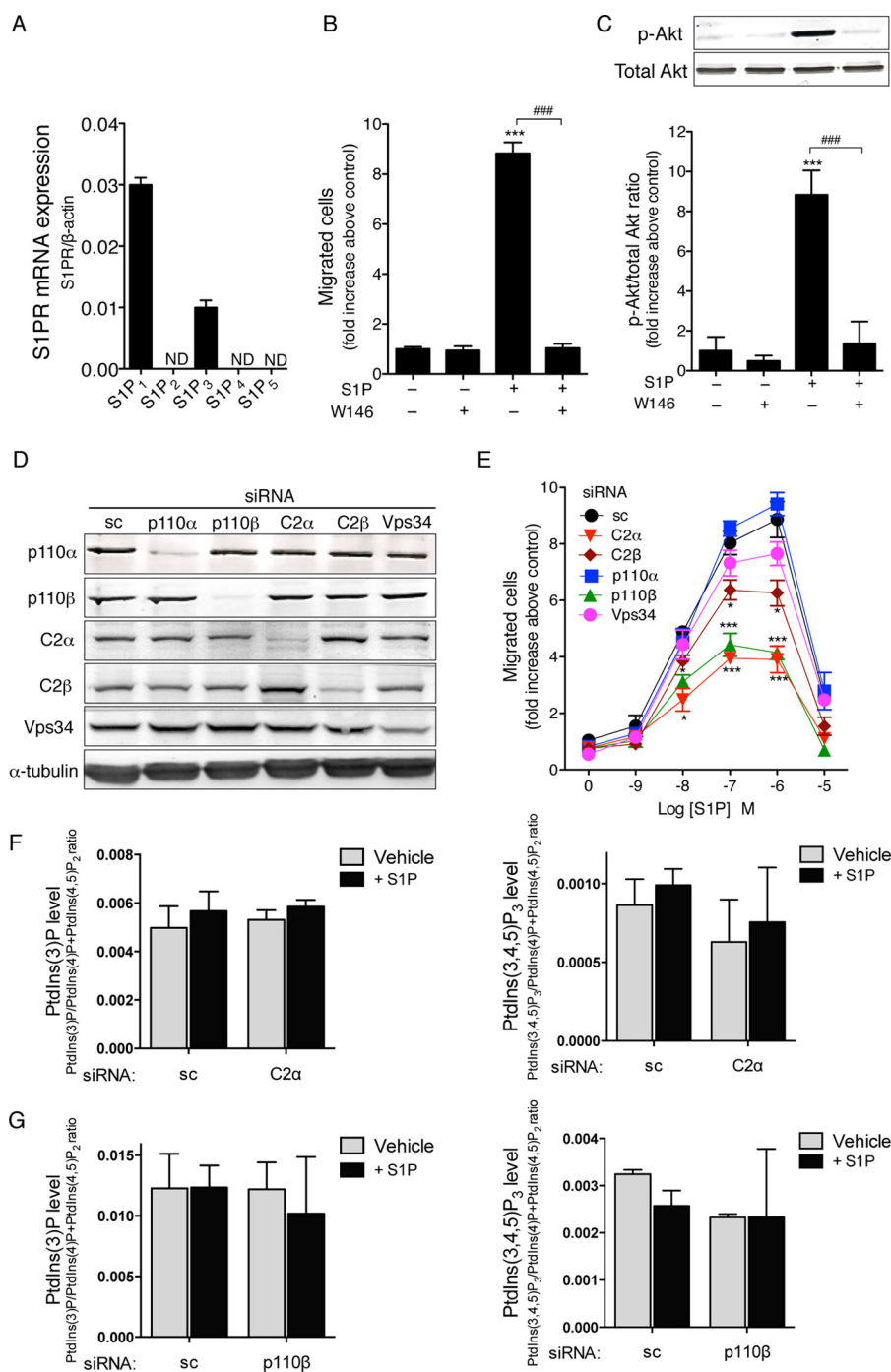


FIGURE 1. S1P stimulates cell migration and Akt activation through S1P₁ in HUVEC. *A*, real-time qPCR analysis of S1P receptor mRNAs in HUVEC. Total RNA was isolated, and qPCR was performed. The mRNA levels of S1P receptors (*S1PR*) are expressed as S1P receptor/ β -actin mRNA ratio. *ND*, non-detectable. *B*, S1P-directed migration of HUVEC is inhibited by an S1P₁-selective antagonist. Transwell cell migration toward S1P was determined using a modified Boyden chamber. Serum-starved HUVEC were placed in the upper chamber. S1P (0.3 μ M) was present only in the lower chamber, whereas the S1P₁ antagonist W146 (3 μ M) was present in both the upper and lower chambers when indicated. *C*, S1P-induced Akt phosphorylation is inhibited by an S1P₁ antagonist. Serum-starved HUVEC were pretreated or non-pretreated with W146 (3 μ M) for 10 min and stimulated with S1P (0.3 μ M) or not for 2 min, followed by Western blot analysis using anti-phospho-Akt (*p-Akt*; Ser-473) and anti-total Akt antibody. *D*, siRNA-mediated knockdown of PI3K protein expression. HUVEC were transfected with either of C2 α -, C2 β -, p110 α -, p110 β -, and Vps34-specific siRNAs or scrambled (sc) siRNA duplex and 48 h later underwent Western blot analysis using anti-PI3K isoform-specific antibodies. α -Tubulin was analyzed as a loading control. *E*, effects of knockdown of different PI3K isoforms on S1P-induced migration of HUVEC. Various concentrations of S1P were added in the lower chamber. *F* and *G*, HPLC analysis of PtdIns(3)P and PtdIns(3,4,5)P₃. HUVEC that had been transfected with either C2 α -specific (*F*) or p110 β -specific (*G*) siRNAs or scrambled siRNA duplex were metabolically labeled with [³²P]orthophosphate for 4 h, and total cellular lipids were extracted and analyzed for the amounts of PtdIns(3)P and PtdIns(3,4,5)P₃. In *A*, *B*, *C*, *F*, and *G*, *n* = 3, and in *E*, *n* = 4. In *B*, *C*, and *E*, * and *** denote statistical significance at the levels of *p* < 0.05 and *p* < 0.001, respectively, compared with the values in the absence of S1P and W146. In *B* and *C*, ### denotes statistical significance between the indicated groups at the level of *p* < 0.001. Error bars, S.E.

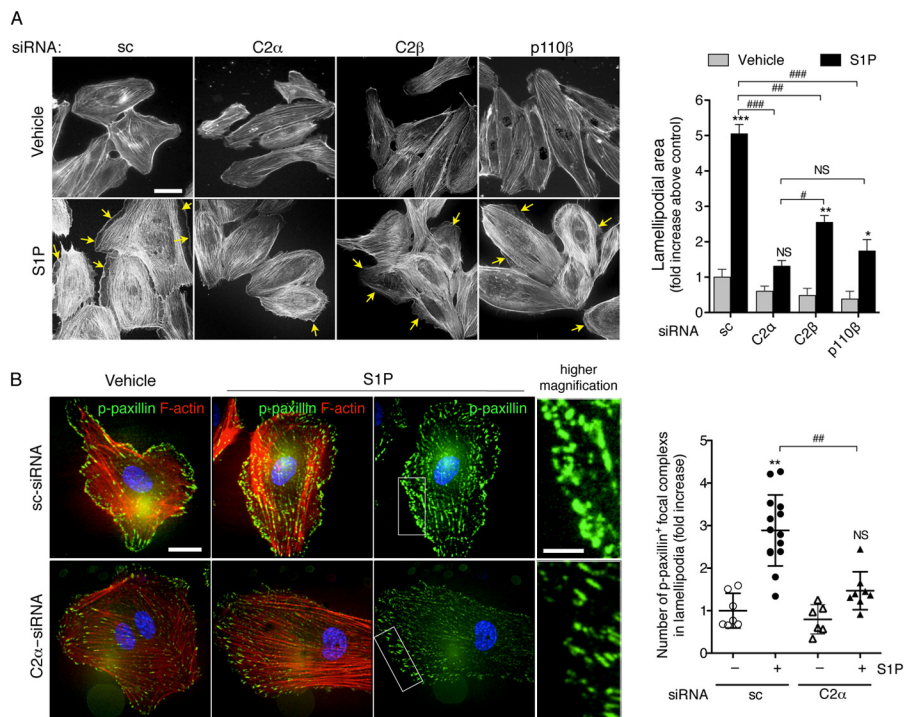


FIGURE 2. PI3K-C2 α knockdown inhibits the formation of lamellipodia and focal complexes. *A*, confocal fluorescent microscopic imaging of F-actin (red) in HUVEC. Cells were transfected with either C2 α -, C2 β -, or p110 β -specific siRNAs or sc-siRNA. Twenty-four h later, the cells were serum-starved overnight and then stimulated with S1P (0.3 μ M) or not for 10 min, followed by AlexaFluor594-conjugated phalloidin staining. Nuclei were stained by DAPI. The yellow arrows indicate lamellipodia. Lamellipodial formation was quantified as described under “Experimental Procedures” (right). $n = 20$ –24 cells. Scale bar, 20 μ m. *B*, immunofluorescent staining of phosphopaxillin (p-paxillin (Tyr-118)) (green) and F-actin (red) in HUVEC. Serum-starved cells were transfected and stimulated with S1P or not, as in *A*. Scale bar, 20 μ m. Higher magnification views of the boxed areas are shown in the right panels. Scale bar, 10 μ m. In *A* and *B*, *, **, and *** denote statistical significance at the levels of $p < 0.05$, $p < 0.01$, and $p < 0.001$, respectively, compared with respective non-stimulated control. #, ##, and ### denote statistical significance between the indicated groups at the levels of $p < 0.05$, $p < 0.01$, and $p < 0.001$, respectively. NS, not significant. Error bars, S.E.

S1P-induced Lamellipodium Formation Is Markedly Inhibited in C2 α -depleted HUVEC—Because lamellipodium formation in migrating cells is caused by actin filament reorganization, which is the most crucial process for cell migration (46), we studied the effects of knockdown of PI3K isoforms on S1P-induced lamellipodium formation. S1P induced the robust formation of lamellipodia in sc-siRNA-transfected HUVEC (Fig. 2A). Knockdown of either C2 α , C2 β , or p110 β reduced the formation of lamellipodia. The inhibitory effect of C2 α knockdown was greater compared with that of C2 β knockdown. Migrating cells form focal complexes at lamellipodia, in which phosphorylated paxillin serves as a docking site for clustering of other focal complex proteins (31, 47–49). S1P stimulation increased the number of focal complexes at the lamellipodia of control HUVEC, as determined with anti-phospho-paxillin immunofluorescent staining (Fig. 2B). In C2 α -depleted cells, S1P-induced formation of focal complexes was markedly diminished compared with that in control HUVEC.

Rac1 Activity Is Inhibited in C2 α -depleted HUVEC—The Rho family GTPases function as molecular switches for cytoskeletal reorganization, focal adhesion/complex assembly, and motility (50). S1P induced time-dependent increases in the amounts of GTP-bound, active forms of Rac1 and RhoA in control HUVEC with 2–3.5-fold peak rises over the basal levels (Fig. 3A). The expression of dominant negative Rac1 mutant (Rac1^{N17}) but not dominant negative RhoA mutant (RhoA^{N19}) inhibited S1P-directed cell migration under our experimental conditions, indicating the essential role of Rac1 in S1P-directed

cell migration (Fig. 3B). Because S1P-induced formation of lamellipodia and focal complexes were impaired in C2 α -depleted HUVEC, we studied the effects of knockdown of C2 α and other PI3K isoforms on the activity of Rac1. C2 α depletion markedly suppressed S1P-induced Rac1 activation, and p110 β depletion inhibited Rac1 activation less prominently, whereas knockdown of either C2 β or p110 α failed to inhibit it (Fig. 3, C and D). In contrast, C2 α knockdown did not inhibit S1P-induced Akt phosphorylation, whereas p110 β knockdown strongly suppressed S1P-induced Akt phosphorylation (Fig. 3E). Knockdown of p110 α , C2 β , or Vps34 was without any inhibitory effect on S1P-induced Akt activation. In addition, knockdown of either of these PI3Ks did not alter S1P-induced ERK activation. Because previous studies showed the involvement of Akt in Rac activation (51, 52), we studied the involvement of Akt in S1P-induced Rac activation. The Akt inhibitor strongly inhibited S1P-induced phosphorylation of its downstream target GSK3 β but had no inhibitory effect on Rac1 activation (Fig. 3F). These observations suggest that C2 α and p110 β but not C2 β are involved in regulating Rac1 activity and thereby cell migration.

C2 α Is Required for Rac1 Activation on Endosomes—We investigated the intracellular sites in which active Rac1 is located or in which Rac1 is activated by S1P within HUVEC by using two different techniques. We first performed immunofluorescent staining using anti-active Rac1 (GTP-Rac1) antibody. We tested the specificity of the anti-active Rac1 antibody. The non-transfected HUVEC and the Cell Tracker Green-la-

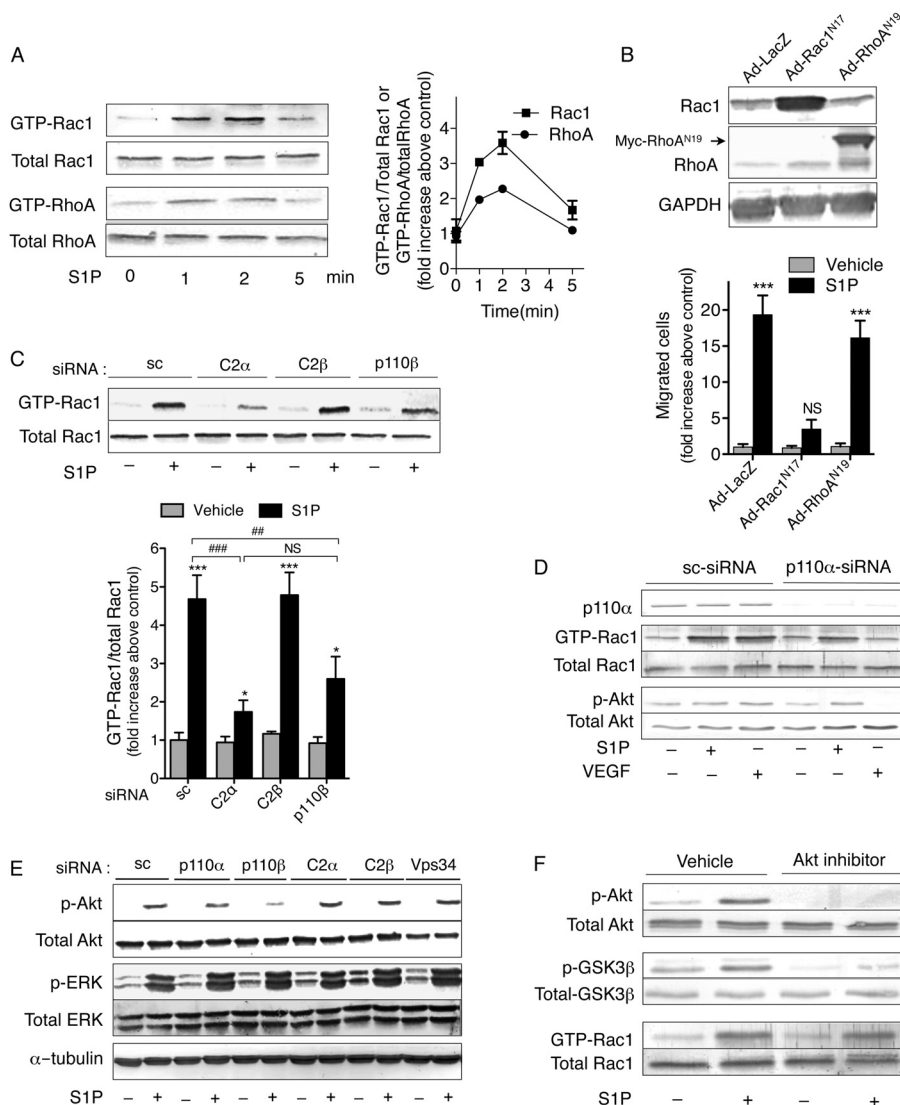


FIGURE 3. PI3K-C2 α knockdown inhibits S1P-induced Rac1 activation. *A*, time-dependent activation of Rac1 and RhoA by S1P in HUVEC. Serum-starved cells were stimulated with S1P (0.3 μ M) for the indicated time periods. The cells were subjected to a pull-down assay for GTP-RhoA and GTP-Rac1. *B*, effects of expression of dominant negative RhoGTPase mutants Rac1^{N17} and RhoA^{N19} on S1P-directed migration of HUVEC. Cells were infected with adenoviruses carrying the cDNAs of LacZ (Ad-LacZ), Rac1^{N17} (Ad-Rac1^{N17}), and Myc-tagged RhoA^{N19} (Ad-RhoA^{N19}); 24 h later serum-starved overnight; and underwent a transwell migration assay. S1P (0.3 μ M) was added to the lower chamber. The protein expression of Rac1^{N17}, Myc-tagged RhoA^{N19}, and GAPDH as endogenous loading control are shown at the top. *C–E*, effects of knockdown of PI3K isoforms on S1P-induced Rac1 activation and Akt phosphorylation. HUVEC were transfected with either C2 α -, C2 β -, p110 α -, or p110 β -specific siRNAs or sc-siRNA. Forty-eight h later, the cells were serum-starved for 6 h and then stimulated with S1P (0.3 μ M) for 2 min, stimulated with VEGF (20 ng/ml) for 10 min, or non-treated, followed by the pull-down assay for GTP-Rac1 (*C*), the pull-down assay for GTP-Rac1, Western blot analysis of phosphorylation of Akt (*p-Akt*) (*D*), and Western blot analysis of phosphorylation of Akt and ERK (*p-ERK*) (*E*). *F*, serum-starved HUVEC were pretreated or not with Akt inhibitor VIII (3 μ M) for 15 min and stimulated with S1P (0.3 μ M) for 2 min, followed by the pull-down assay for GTP-Rac1 and Western blot analysis of phosphorylation of Akt and GSK3 β . In *A* and *B*, $n = 3$, and in *C*, $n = 4$. *D–F* represent three independent experiments. In *B* and *C*, * and *** denote statistical significance at the levels of $p < 0.05$ and $p < 0.001$, respectively, compared with respective non-stimulated control. In *C*, ## and ### denote statistical significance between the indicated groups at the levels of $p < 0.01$ and $p < 0.001$, respectively. Error bars, S.E.

beled HUVEC transfected with Rac1^{N17}, which remains bound to a guanine nucleotide exchange factor and thereby prevents GTP loading of endogenous Rac1, were mixed and cultured. The mixed cell culture was stimulated with S1P and underwent anti-active Rac1 immunofluorescent staining. The non-transfected cells were intensely stained with anti-active Rac1, whereas Rac1^{N17}-transfected cells were nearly negative for anti-active Rac1 staining (Fig. 4*A*), indicating that the antibody specifically detected active Rac1. The non-stimulated, sc-siRNA-transfected HUVEC showed anti-active Rac1 staining in the plasma membrane, particularly lamellipodia, and in the intracellular compartment, the latter being stained in a granular or fine

speckled pattern (Fig. 4*B*, top). S1P-stimulated cells displayed much more intense staining in both the lamellipodial area and the intracellular compartment compared with non-stimulated cells. Knockdown of C2 α markedly attenuated anti-active Rac1 staining in both the lamellipodia and the intracellular compartment of non-stimulated and S1P-stimulated cells.

The intracellular granular staining of active Rac1 suggested that Rac1 activation might occur in endosomes, which are relatively rich in PtdIns(3)P (2, 4). Therefore, we studied whether active Rac1 and PtdIns(3)P co-localized or not by determining the localization of active Rac1 and fluorescence of the PtdIns(3)P-specific probe GFP-tagged 2xFYVE domain.

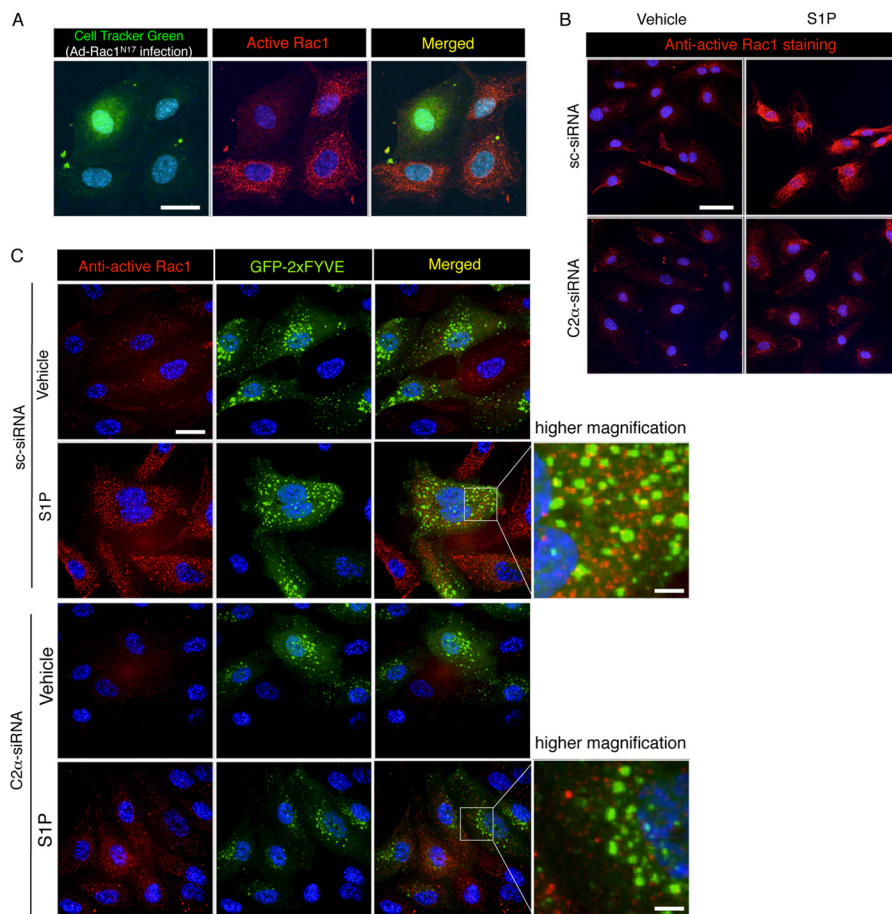


FIGURE 4. **PI3K-C2 α knockdown inhibits S1P-induced Rac1 activation in the intracellular vesicular compartment in HUVEC.** *A*, effects of Rac1^{N17} expression on anti-active Rac1 immunofluorescent staining in HUVEC. Cells were infected with Ad-Rac1^{N17}, 24 h later labeled with Cell Tracker Green, and mixed with Ad-LacZ-infected control HUVEC at a 1:1 ratio. The mixed cells were plated and cultured overnight. Then the cells were serum-starved for 6 h and stimulated by S1P (0.3 μ M) for 2 min, followed by immunofluorescent staining for GTP-Rac1 using anti-active Rac1-specific antibody. *Scale bar*, 20 μ m. *B*, immunofluorescent staining of active Rac1 in control and C2 α -depleted HUVEC. Cells transfected with either C2 α -siRNA or sc-siRNA were serum-starved overnight and stimulated with S1P (0.3 μ M) or not for 2 min, followed by immunofluorescent staining for GTP-Rac1 as in *A*. *Scale bar*, 20 μ m. *C*, effects of C2 α -knockdown on anti-active Rac1 immunostaining and GFP-2xFYVE distribution in HUVEC. Cells were transfected with GFP-2xFYVE expression vector, cultured overnight, and then serum-starved for 6 h. The cells were stimulated with S1P (0.3 μ M) or not for 2 min and underwent anti-active Rac1 immunofluorescent staining. *Scale bar*, 20 μ m. Higher magnification of the boxed area in the merged view is also shown. *Scale bar*, 5 μ m.

HUVEC were transfected with the expression vector for GFP-tagged 2xFYVE domain and subjected to anti-active Rac1 immunofluorescent staining. In S1P-stimulated sc-siRNA-transfected HUVEC, a significant portion of the anti-active Rac1 signal overlapped with the GFP-2xFYVE signal, indicating that at least a part of S1P-activated Rac1 exists in PtdIns(3)-P-enriched endosomes (Fig. 4C). S1P stimulation of sc-siRNA-transfected HUVEC did not alter the number, distribution, or motility of GFP-2xFYVE⁺ vesicles. C2 α knockdown substantially reduced the number of GFP-2xFYVE⁺ endosomes and anti-active Rac1 signal, resulting in a marked decrease of active Rac1 in GFP-2xFYVE⁺ endosomes.

We determined cellular sites of Rac1 activation in HUVEC by adopting a FRET imaging technique. Rac1 was activated in both the intracellular vesicular compartment and the plasma membrane, particularly membrane ruffles, in S1P-stimulated sc-siRNA-treated HUVEC (Fig. 5A and supplemental Movie 1). There was the tendency that Rac1 activation was first observed in the membrane ruffles and then in the intracellular vesicles. C2 α depletion markedly suppressed Rac1-FRET signals in both the plasma membrane and the intracellular compartment in

non-stimulated and S1P-stimulated HUVEC (Fig. 5A and supplemental Movie 2). In S1P-stimulated sc-siRNA-treated HUVEC that were co-transfected with the expression vectors for mRFP-tagged 2xFYVE domain and the Rac1-FRET probe, a substantial portion of the intracellular Rac1-FRET signals were co-localized with RFP-2xFYVE signals (Fig. 5, *B* (top left and bottom (white and yellow arrowheads, respectively)) and *C*). The Rac1-FRET signal was also intense at cell-cell contacts (Fig. 5B (bottom left, red arrowheads)). However, Rac1-FRET signal⁺ cell-cell contacts were negative for RFP-2xFYVE. C2 α depletion greatly attenuated Rac1-FRET signals in the RFP-2xFYVE⁺ endosomes (Fig. 5, *B* (top middle and bottom) and *C*), indicating that C2 α is essential for Rac1 activation in the PtdIns(3)P-enriched endosomes and the plasma membrane. In contrast, knockdown of p110 β did not reduce RFP-2xFYVE⁺ vesicles or intracellular vesicular Rac1-FRET signals but attenuated Rac1-FRET signal in the plasma membrane (Fig. 5, *B* (top right and bottom) and *C*).

S1P-induced Internalization of S1P₁ Is Dependent on C2 α and Required for Rac1 Activation and Migration in HUVEC—We studied the role of C2 α in S1P₁ internalization upon S1P

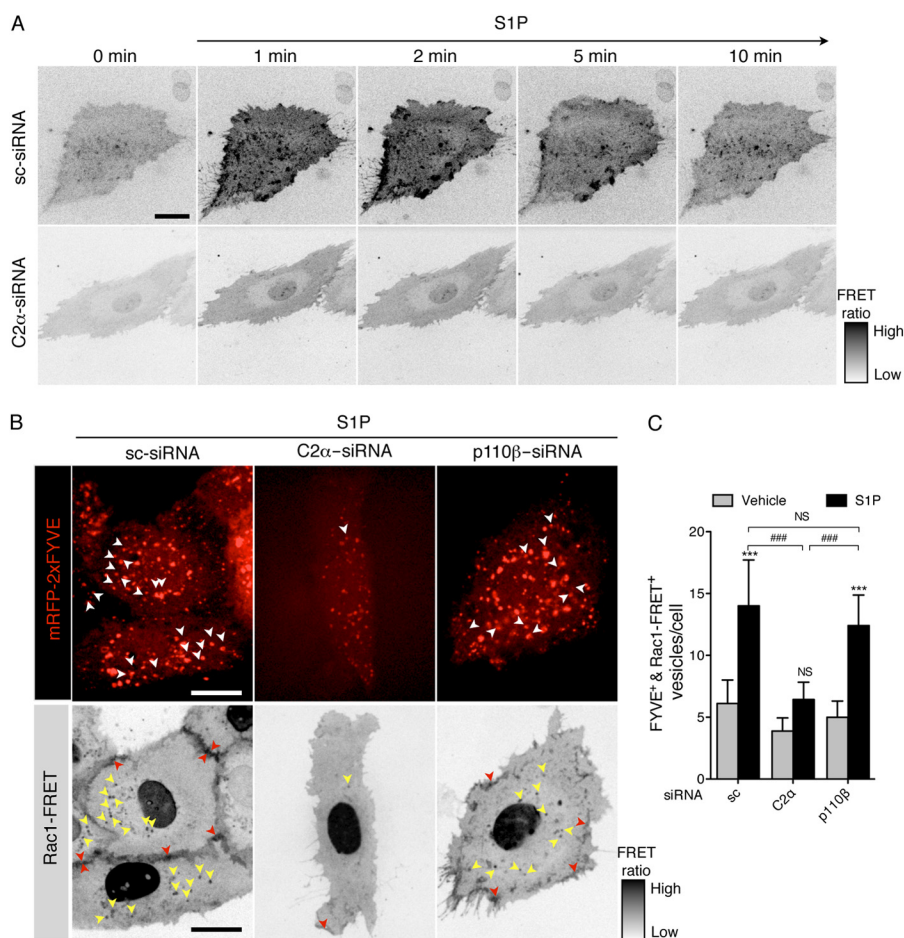


FIGURE 5. FRET imaging of inhibition by PI3K-C2 α knockdown of S1P-induced Rac1 activation in HUVEC. *A*, FRET imaging of Rac1 activation in control and C2 α -depleted HUVEC. Cells that were co-transfected with pRaichu-Rac1 and either C2 α -siRNA or sc-siRNA were cultured overnight and then serum-starved for 6 h, followed by FRET imaging. The cells were stimulated with S1P (0.3 μ M). *B*, co-localization of the Rac1-FRET signal and mRFP-2xFYVE signal. Cells co-transfected with pRaichu-Rac1 and the mRFP-2xFYVE expression vector were cultured overnight and then serum-starved for 6 h. The cells were stimulated with S1P (0.3 μ M) for 2 min with fluorescent microscopic observations. The white arrowheads in the 2xFYVE images and the yellow arrowheads in the FRET images are overlapped. The red arrowheads indicate Rac1 activation at cell-cell contacts. *C*, quantification of mRFP-2xFYVE⁺ and Rac1-FRET signal⁺ vesicles. $n = 12$ –20 cells. Scale bar, 20 μ m. In *C*, *** denotes statistical significance at $p < 0.001$ compared with non-stimulated control, and ### denotes statistical significance between the indicated groups at a level of $p < 0.001$. NS, not significant. Error bars, S.E.

stimulation in HUVEC co-transfected with the expression vectors for mRFP-S1P₁ and GFP-2xFYVE. S1P stimulation induced robust internalization of S1P₁ with substantial co-localization of the internalized S1P₁ and the intracellular GFP-2xFYVE signals in sc-siRNA-transfected control HUVEC (Fig. 6A and supplemental Movie 3). In C2 α -depleted cells, S1P-induced S1P₁ internalization was much attenuated (Fig. 6A and supplemental Movie 4), indicating that C2 α is required for S1P₁ internalization. In contrast to C2 α -depleted cells, S1P induced the internalization of S1P₁ in p110 β -depleted cells as well as in control HUVEC, indicating that p110 β is not required for S1P-induced S1P₁ internalization. In HUVEC co-transfected with sc-siRNA and the expression vectors for mRFP-S1P₁ and the Rac1-FRET probe, S1P induced time-dependent increases in Rac1-FRET signals in the endosomes and the plasma membrane with S1P₁ internalization (Fig. 6B and supplemental Movie 1). At least a portion of S1P-induced FRET signals co-localized with mRFP-S1P₁ in the endosomes as well as in the plasma membrane. C2 α depletion markedly suppressed S1P₁ internalization as well as Rac1-FRET signal (Fig. 6B and supplemental Movie 2).

We further investigated the role of S1P₁ internalization in S1P₁-mediated cell signaling and migration by studying the effects of dynasore, an inhibitor of dynamin, which is a molecule essential for vesicle formation in endocytosis (53). Treatment of HUVEC with dynasore strongly inhibited S1P-induced internalization of S1P₁ and reduced GFP-2xFYVE⁺ vesicles (compare Fig. 7A with Fig. 6A). Cell migration is also inhibited by dynasore treatment (Fig. 7B). Similar to the effects of C2 α knockdown, dynasore inhibited S1P-induced activation of Rac1 but not of Akt or ERK (Fig. 7, C and D). These observations lend further support for the notion that the internalized S1P₁ activates Rac1 on endosomes and thereby cell migration.

C2 α Is Essential for Tube Formation of HUVEC—We studied the role of C2 α in S1P-induced tube formation of HUVEC on Matrigel. Depletion of C2 α but not C2 β in HUVEC inhibited S1P-induced tube formation (Fig. 8A). Knockdown of p110 β partially inhibited S1P-induced tube formation. S1P-induced tube formation was dependent on Rac1, as demonstrated by abolition of tube formation by adenovirus-mediated expression of Rac1^{N17} (Fig. 8B). Finally, dynasore abolished S1P-induced

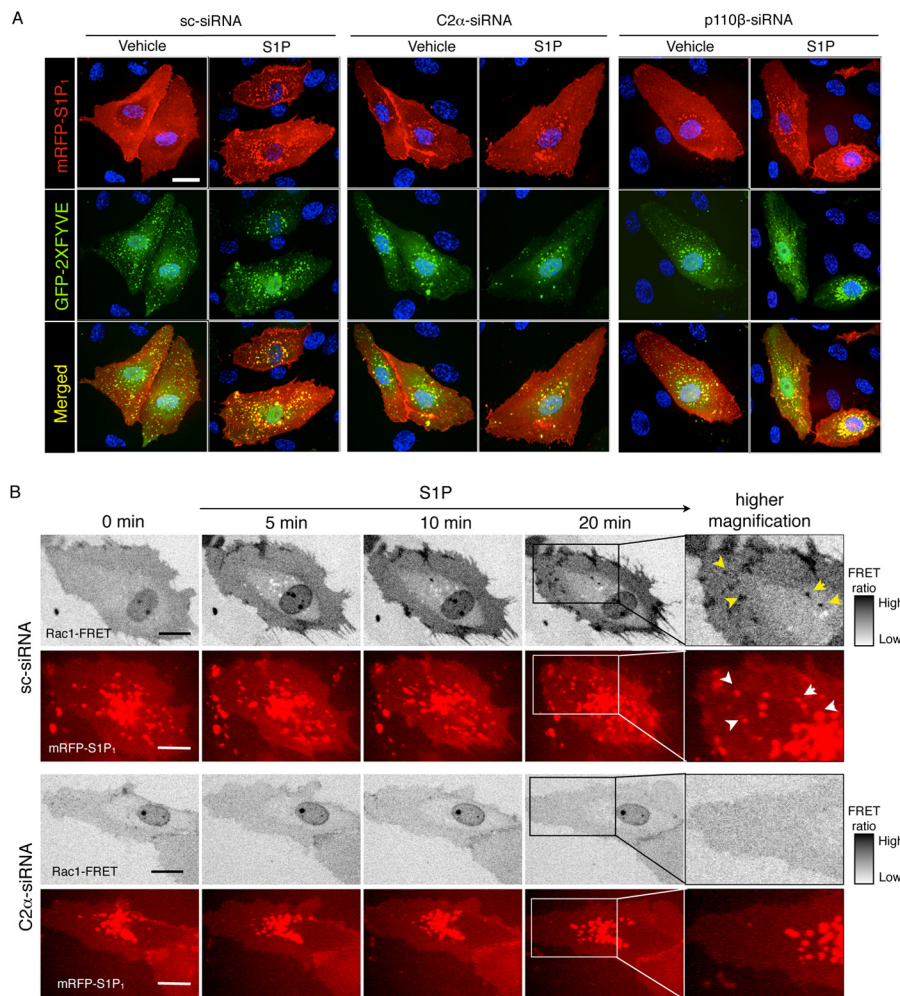


FIGURE 6. S1P induces S1P₁ internalization into GFP-2xFYVE⁺ vesicles in a PI3K-C2 α -dependent manner and activates Rac1 in S1P₁⁺ vesicles in HUVEC. *A*, effects of knockdown of C2 α and p110 β on S1P-induced S1P₁ internalization. Cells were co-transfected with the expression vectors for mRFP-S1P₁, GFP-2xFYVE, and either C2 α -siRNA, p110 β -siRNA, or sc-siRNA. Twenty-four h later, the cells were serum-starved overnight and stimulated with S1P (0.3 μ M) for 30 min. The cells were observed with a confocal fluorescent microscope as described under “Experimental Procedures.” *B*, co-localization of mRFP-S1P₁ and the Rac1-FRET signal (white (bottom) and yellow (top) arrowheads, respectively). Cells co-transfected with mRFP-S1P₁ expression vector and pRaichu-Rac1 were cultured overnight and then serum-starved for 6 h. The cells were stimulated with S1P (0.3 μ M) for 30 min with fluorescent microscopic observations. Scale bar, 20 μ m.

tube formation (Fig. 8C), indicating that S1P-induced tube formation was dependent on an endocytic process.

DISCUSSION

The present study demonstrates that class II PI3K member C2 α is essential for S1P₁-mediated EC migration, capillary-like tube formation, and particular cell signaling (*i.e.* Rac1 activation, which is a signal crucial for cell motility and endothelial morphogenesis) in a manner different from class I PI3K. We show for the first time that S1P₁-mediated Rac1 activation occurs not only in the plasma membrane but also on endosomes and requires C2 α . The endosomes where Rac1 activation occurs in response to S1P stimulation are enriched in PtdIns(3)P, a major product of C2 α , and bear the internalized S1P₁. S1P-induced S1P₁ internalization requires C2 α . Pharmacological blockade of S1P₁ internalization markedly inhibits activation of Rac1 but not Akt or ERK and thereby suppresses cell migration and tube formation. Thus, C2 α plays a thus far unrecognized, distinct role in S1P₁-mediated endothelial

migration and morphogenesis by engaging in S1P₁ internalization and subsequent signaling on endosomes.

C2 α ; another class II member, C2 β ; and also class III Vps34 all generate PtdIns(3)P, which is mainly accumulated in the intracellular membranes, including early endosomes, multivesicular bodies/late endosomes, phagosomes, and the Golgi apparatus (1, 4, 13). The localized enrichment of PtdIns(3)P provides the platform for recruiting effector proteins containing FYVE, PX, and PH domains, thus regulating membrane trafficking and controlling signal transduction, cytoskeletal reorganization, phagocytosis, and autophagy (54). Our data indicate that C2 α is involved in S1P₁-mediated, selected signaling through controlling vesicular trafficking-dependent processes; under the condition in which S1P-induced internalization of S1P₁ is blocked by either C2 α depletion or dynasore (dynamin inhibitor) treatment, S1P-induced activation of Rac1 but not ERK or Akt is greatly suppressed (Figs. 3C and 7, C and D). Furthermore, Rac1 activation in the intracellular compartment is localized to S1P₁⁺ and FYVE⁺ vesicles (Figs. 5B and

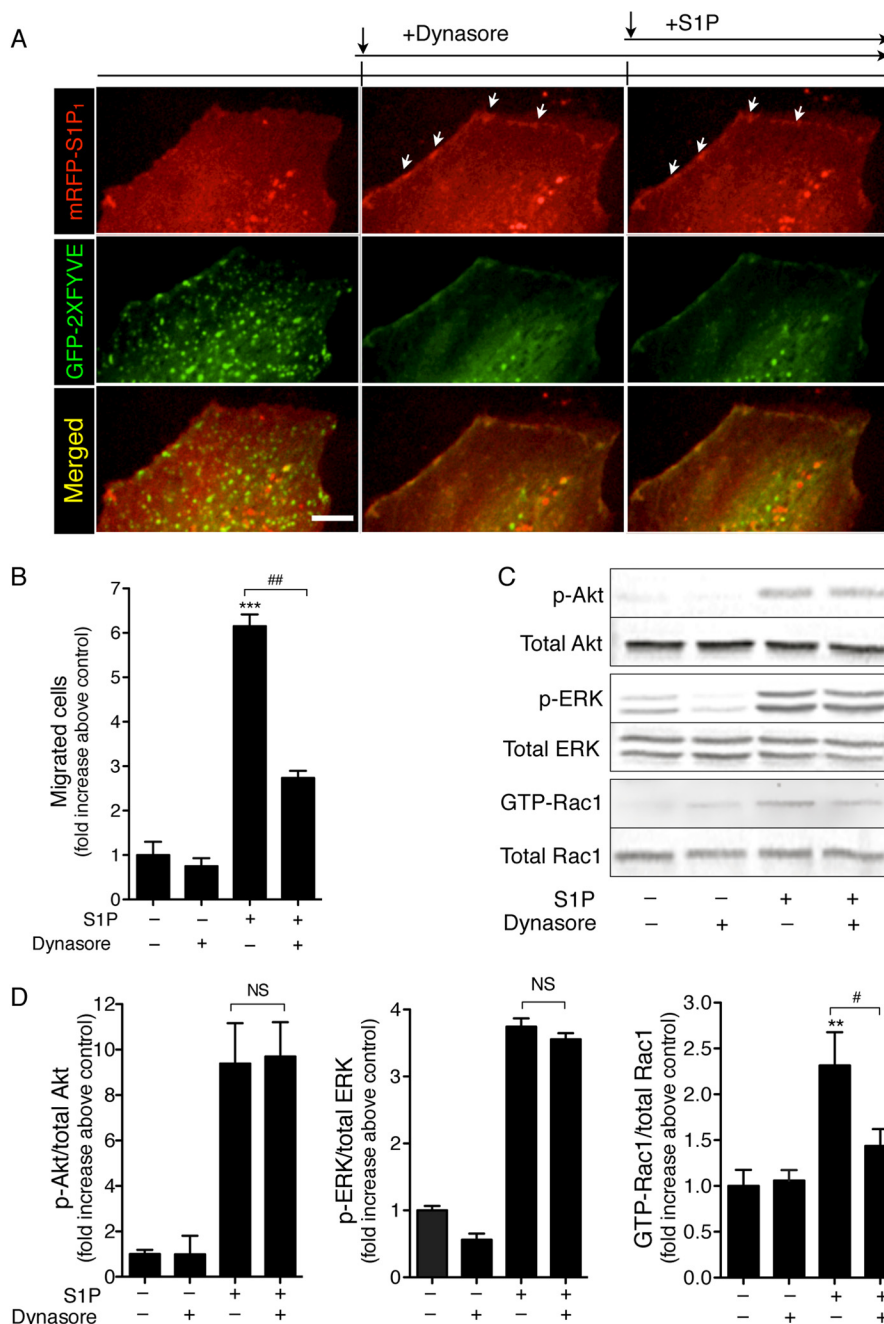


FIGURE 7. An inhibitor of endocytosis blocks S1P-induced S1P₁ internalization, cell migration, and Rac1 activation in HUVEC. *A*, effects of dynasore on S1P-induced S1P₁ internalization. Cells were co-transfected with the expression vectors for mRFP-S1P₁ and GFP-2xFYVE, serum-starved overnight, and stimulated with S1P (0.3 μ M) or not for 30 min with or without dynasore (40 μ M) pretreatment for 1 h. The cells were observed with a confocal fluorescent microscope as in Fig. 6A. Scale bar, 20 μ m. *B*, effects of dynasore on S1P-directed migration of HUVEC. Serum-starved cells were pretreated with dynasore (40 μ M) or not for 1 h and then underwent a transwell migration assay. S1P (0.3 μ M) was added in the lower chamber. *C*, effects of dynasore on S1P-induced Rac1 activation and phosphorylation of Akt (*p*-Akt) and ERK (*p*-ERK). Cells were treated as in *B* and stimulated with S1P (0.3 μ M) for 2 min. *D*, quantified data of phospho-Akt (*p*-Akt), phospho-ERK (*p*-ERK), and GTP-Rac1. *n* = 3. In *B* and *D*, ** and *** denote statistical significance at the levels of $p < 0.01$ and $p < 0.001$, respectively, compared with respective non-treated control. # and ## denote statistical significance between the indicated groups at the levels of $p < 0.05$ and $p < 0.01$, respectively. NS, not significant. Error bars, S.E.

6B). Thus, very likely, internalized S1P₁ on PtdIns(3)P-enriched endosomes is engaged in Rac1 activation. Because S1P-non-stimulated, C2 α -depleted cells display a marked decrease in the number of FYVE⁺ vesicles and inhibition of their motility (13) and S1P stimulation does not alter the abundance of FYVE⁺ vesicles (Figs. 4C and 6A), it is suggested that the basal level of vesicular PtdIns(3)P provided by a constitutive activity of C2 α plays a crucial role in S1P-induced endosomal signaling in

HUVEC. We found that knockdown of C2 α but not C2 β or Vps34 reduces the number of FYVE⁺ vesicles in HUVEC (13).⁴ In the present study, we did not observe a decrease in the total cellular level of PtdIns(3)P in C2 α -depleted HUVEC (Fig. 1F). This finding suggests that a majority of total cellular PtdIns(3)P

⁴ K. Biswas, unpublished observation.

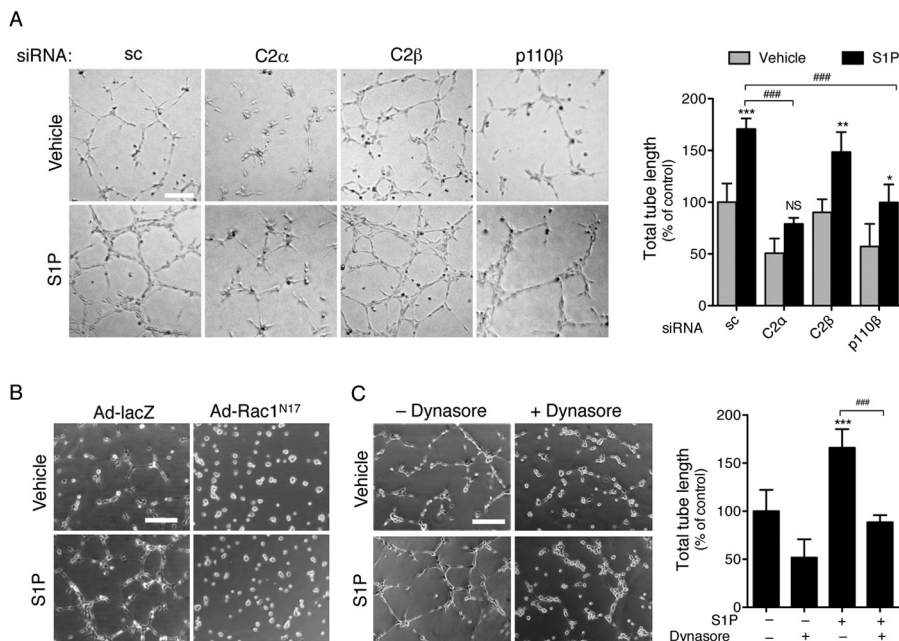


FIGURE 8. PI3K-C2 α knockdown and dynasore inhibit S1P-induced tube formation in HUVEC. *A*, effects of knockdown of PI3K isoforms on tube formation. Cells were co-transfected with either C2 α -siRNA, C2 β -siRNA, p110 β -siRNA, or sc-siRNA and 24 h later were serum-starved overnight. The cells were seeded on growth factor-reduced Matrigel in a 24-well plate containing 0.3 μ M S1P and allowed to form tube-like structures for 6 h. *Right*, quantified data of tube length. $n = 4$. *Scale bar*, 200 μ m. *B*, effects of the expression of a dominant negative Rac1 mutant on S1P-induced tube formation. Cells were infected with either Ad-LacZ or Ad-Rac1^{N17} as in Fig. 3B and 24 h later were serum-starved overnight, followed by tube formation assay as in *A*. *C*, effects of dynasore on S1P-induced tube formation. Cells were pretreated with dynasore or not for 1 h and underwent tube formation assay as in *A*. *Scale bar*, 200 μ m. *Right*, quantified data of tube length. $n = 3$. In *A* and *C*, *, **, and *** denote statistical significance at the levels of $p < 0.05$, $p < 0.01$, and $p < 0.001$, respectively, compared with respective non-stimulated control. ### denotes statistical significance between the indicated groups at a levels of $p < 0.001$. NS, not significant. *Error bars*, S.E.

in HUVEC is synthesized by other PI3Ks, such as Vps34 and C2 β , and that C2 α may produce PtdIns(3)P in the particular compartments, including early endosomes and the *trans*-Golgi network. We did not observe an S1P-induced increase in PtdIns(3,4,5)P₃ level (Fig. 1, *F* and *G*). This could be because S1P might increase the level of PtdIns(3,4,5)P₃ only in a subdomain of the plasma membrane, and our method for determining PtdIns(3,4,5)P₃ in HUVEC might not have enough sensitivity to detect a localized increase in this lipid in the plasma membrane because of poor metabolic labeling of cellular lipids in this type of cells.

Endocytosis of cell surface receptors has been viewed as a mechanism of signal termination by internalizing and degrading receptors (55, 56). However, recent studies demonstrate that endosomes serve as platforms to assemble membrane receptors and their downstream signaling molecules to generate spatially localized signals (56). For example, Rac activation by certain receptor tyrosine kinase ligands is shown to occur on endosomes, which requires the recruitment of the adaptor protein APPL, the Rac-GEF Tiam-1, and plasma membrane-anchored GDP-bound Rac1 (34, 35). In many cases of G protein-coupled receptor signaling, Rac activation by chemotactic ligands is mediated largely by G_i and through the action of guanine nucleotide exchange factors, such as P-Rex1 (57, 58). The chemotactic receptor S1P₁ is exclusively coupled to G_i, and S1P₁-mediated Rac1 activation is indeed G_i-dependent (36, 59). It remains to be defined how adaptors and a Rac-GEF assemble in the PtdIns(3)P-enriched S1P₁⁺ endosomes to activate the Rac pathway. A previous study showed that the S1P₁ agonist FTY720-phosphate produced persistent S1P₁ endocytosis and

a prolonged reduction in cellular cyclic AMP level. This study suggests that, besides the Rac1 pathway, endosomal S1P₁ also signals to inhibit adenylate cyclase (60).

Previous studies showed that C2 β is involved in migration of non-endothelial cells (61–63). The results in those studies differ from our observations in EC migration in several aspects (*i.e.* in the regulation of the PI3K activities, the distribution of the PI3Ks, and the distribution of their product PtdIns(3)P). Migration of ovarian and uterine cervical tumor cells stimulated by the lipid mediator lysophosphatidic acid in a wound healing assay was dependent on C2 β but not C2 α with increased production of PtdIns(3)P; lysophosphatidic acid stimulation induced translocation of C2 β and GFP-2xFYVE probe from the intracellular compartment to the plasma membrane, the latter of which was abolished by knockdown of C2 β but not C2 α (61). In epidermoid carcinoma cells, C2 β was found to associate with epidermal growth factor (EGF) receptor by forming a complex with adaptor proteins and the Rac/Ras-GEF SOS, and EGF stimulated C2 β activity as well as Rac1 activity. Overexpression of either wild-type C2 β or a dominant negative C2 β mutant enhanced or suppressed cell migration, respectively. Moreover, C2 β overexpression enhanced EGF-induced Rac1 activation, whereas that of the dominant negative C2 β mutant inhibited Rac1 activation (63). In addition, C2 β overexpression in human kidney cells stimulated cell migration with activation of Cdc42 but not Rac1, and endogenous C2 β was localized in both lamellipodia and intracellular vesicles (62). In our study, although transwell migration of HUVEC toward S1P was inhibited by knockdown of either C2 α or C2 β , the C2 β dependence of cell migration was much less in magnitude compared with that of

C2 α (Fig. 1E). Consistently, C2 β knockdown failed to inhibit S1P-induced Rac1 activation in HUVEC, unlike C2 α knockdown (Fig. 3C). In addition, Vps34, which exclusively produces PtdIns(3)P, did not at all inhibit S1P-directed migration (Fig. 1E). Our recent study (13) also showed that C2 α but not C2 β or Vps34 decreased GFP-2xFYVE⁺ endosomes in non-stimulated HUVEC and prevented VEGF-induced tube formation. Differently from the case of the tumor cells in which C2 β is responsible for stimulus-induced increase in PtdIns(3)P in the plasma membrane, C2 α rather contributes to PtdIns(3)P level in the intracellular vesicular compartment under non-stimulated basal conditions in HUVEC (Figs. 4C and 6A). Consistent with this notion, S1P did not induce translocation to the plasma membrane of C2 α in HUVEC.⁴ These observations together suggest that C2 α is probably located in a different endosomal compartment from C2 β and Vps34, undergoes distinct regulation, and thereby serves specialized functions in HUVEC. Of note is the structural difference between C2 α and C2 β ; only C2 α possesses a clathrin-binding site (8). However, the possibility is not excluded that the functions of C2 α and C2 β are partially redundant in HUVEC. It is possible that the apparent discrepancies regarding the roles of class II PI3K in cell migration between the previous studies and our study could be explained by cell type-specific difference in relative expression levels of these two class II PI3K, cell type- and PI3K isoform-specific differences in the regulatory mechanisms for the activities of the PI3K and a cell type-specific difference in the intracellular localization of the PI3K. Further study is required for defining whether and to what extent the functions of these PI3Ks are overlapping or distinct in ECs and other cells.

S1P₁-mediated cell migration is dependent on not only C2 α but also p110 β (Fig. 1E). S1P-induced Rac1 activation is also dependent on p110 β (Fig. 3C). This is consistent with the recent observations that G protein-coupled receptors are coupled to p110 β rather than p110 α (1, 45, 64). p110 β produces mainly PtdIns(3,4,5)P₃, unlike class II and III PI3Ks (1). PtdIns(3,4,5)P₃ serves to recruit a Rac-GEF to the membrane mainly through interacting with a PH domain of a Rac-GEF and to activate it probably together with G $\beta\gamma$ (57). Impressively, p110 β knockdown substantially attenuates Rac1 activation in the plasma membrane but has little effect on endosomal Rac1 activation (Fig. 5B (bottom)), suggesting that an increase in PtdIns(3,4,5)P₃ level may not be necessary for the recruitment and assembly of a Rac-GEF on signaling endosomes. In contrast, C2 α knockdown inhibits S1P-induced Rac1 activation in both the plasma membrane and endosomes (Fig. 5B, middle). As evaluated with GFP-2xFYVE labeling, PtdIns(3)P is accumulated mainly in the endosomes and other vesicular structures but not the plasma membrane (Figs. 4C and 6A). Moreover, this distribution pattern of PtdIns(3)P is not changed by S1P stimulation. Hence, the dependence of plasmalemmal Rac1 activation on C2 α may indicate that one or more processes of Rac1 activation in the plasma membrane (e.g. delivery and assembly of adaptors and a Rac-GEF to the plasma membrane and also recycling of S1P₁) require C2 α .

C2 α could be involved in cell migration through not only facilitating the assembly of Rac1-activating machinery on endosomes but through other mechanisms involving endosomal

trafficking; C2 α may be engaged in the transport of Rac1 activated on endosomes to the front of migrating cells to ensure the formation of actin-based protrusions (34, 35, 64). Integrins, lipid raft domains, and other small GTPases, such as Arf6, may also traffic to the leading edge, promoting the formation of the focal complex/adhesion and actin polymerization. Also, at the rear of the cells, focal adhesion disassembly and cell contraction may involve endosomal platforms through the assembly of Rho and Rho kinase.

The present study demonstrates for the first time that C2 α is involved in selective cell signaling on endosomes. Our data show that C2 α is functionally essential for S1P-induced EC migration and morphogenesis, suggesting that the crucial role of C2 α in angiogenesis (13) may be in part explained by the C2 α requirement in the S1P actions on ECs. We recently showed that C2 α also plays an indispensable role in maintaining endothelial barrier function (13). It is known that S1P exerts a barrier-protective effect through regulating Rac1 (21, 55). Therefore, C2 α -dependent endosomal Rac1 activation may also serve as a signal to enhance vascular barrier protection. Because angiogenesis and barrier integrity are important vascular functions in both physiology and pathophysiology, our study opens a new avenue for establishing a therapeutic strategy to regulate physiological and pathological vascular processes by controlling C2 α .

Acknowledgment—We thank C. Hirose for secretarial assistance.

REFERENCES

1. Vanhaesebroeck, B., Guillermet-Guibert, J., Graupera, M., and Bilanges, B. (2010) The emerging mechanisms of isoform-specific PI3K signalling. *Nat. Rev. Mol. Cell Biol.* **11**, 329–341
2. Sasaki, T., Takasuga, S., Sasaki, J., Kofuji, S., Eguchi, S., Yamazaki, M., and Suzuki, A. (2009) Mammalian phosphoinositide kinases and phosphatases. *Prog. Lipid Res.* **48**, 307–343
3. Vanhaesebroeck, B., Stephens, L., and Hawkins, P. (2012) PI3K signalling. The path to discovery and understanding. *Nat. Rev. Mol. Cell Biol.* **13**, 195–203
4. Lindmo, K., and Stenmark, H. (2006) Regulation of membrane traffic by phosphoinositide 3-kinases. *J. Cell Sci.* **119**, 605–614
5. Mazza, S., and Maffucci, T. (2011) Class II phosphoinositide 3-kinase C2 α . What we learned so far. *Int. J. Biochem. Mol. Biol.* **2**, 168–182
6. Falasca, M., Hughes, W. E., Dominguez, V., Sala, G., Fostira, F., Fang, M. Q., Cazzolli, R., Shepherd, P. R., James, D. E., and Maffucci, T. (2007) The role of phosphoinositide 3-kinase C2 α in insulin signaling. *J. Biol. Chem.* **282**, 28226–28236
7. Falasca, M., and Maffucci, T. (2012) Regulation and cellular functions of class II phosphoinositide 3-kinases. *Biochem. J.* **443**, 587–601
8. Gaidarov, I., Zhao, Y., and Keen, J. H. (2005) Individual phosphoinositide 3-kinase C2 α domain activities independently regulate clathrin function. *J. Biol. Chem.* **280**, 40766–40772
9. Gaidarov, I., Smith, M. E., Domin, J., and Keen, J. H. (2001) The class II phosphoinositide 3-kinase C2 α is activated by clathrin and regulates clathrin-mediated membrane trafficking. *Mol. Cell* **7**, 443–449
10. Domin, J., Gaidarov, I., Smith, M. E., Keen, J. H., and Waterfield, M. D. (2000) The class II phosphoinositide 3-kinase PI3K-C2 α is concentrated in the trans-Golgi network and present in clathrin-coated vesicles. *J. Biol. Chem.* **275**, 11943–11950
11. Wang, Y., Yoshioka, K., Azam, M. A., Takuwa, N., Sakurada, S., Kayaba, Y., Sugimoto, N., Inoki, I., Kimura, T., Kuwaki, T., and Takuwa, Y. (2006) Class II phosphoinositide 3-kinase α -isoform regulates Rho, myosin phosphatase, and contraction in vascular smooth muscle. *Biochem. J.* **394**,

- 581–592
12. El Sheikh, S. S., Domin, J., Tomtitchong, P., Abel, P., Stamp, G., and Lalani, E.-N. (2003) Topological expression of class IA and class II phosphoinositide 3-kinase enzymes in normal human tissue is consistent with a role in differentiation. *BMC Clin. Pathol.* **3**, 4
 13. Yoshioka, K., Yoshida, K., Cui, H., Wakayama, T., Takuwa, N., Okamoto, Y., Du, W., Qi, X., Asanuma, K., Sugihara, K., Aki, S., Miyazawa, H., Biswas, K., Nagakura, C., Ueno, M., Iseki, S., Schwartz, R. J., Okamoto, H., Sasaki, T., Matsui, O., Asano, M., Adams, R. H., Takakura, N., and Takuwa, Y. (2012) Endothelial PI3K-C2 α , a class II PI3K, has an essential role in angiogenesis and vascular function. *Nat. Med.* **18**, 1560–1569
 14. Spiegel, S., and Milstien, S. (2011) The outs and the ins of sphingosine-1-phosphate in immunity. *Nat. Rev. Immunol.* **11**, 403–415
 15. Blaho, V. A., and Hla, T. (2011) Regulation of mammalian physiology, development, and disease by the sphingosine 1-phosphate and lysophosphatidic acid receptors. *Chem. Rev.* **111**, 6299–6320
 16. Ishii, I., Fukushima, N., Ye, X., and Chun, J. (2004) Lysophospholipid receptors. Signaling and Biology. *Annu. Rev. Biochem.* **73**, 321–354
 17. Takuwa, Y., Okamoto, Y., Yoshioka, K., and Takuwa, N. (2012) Sphingosine-1-phosphate signaling in physiology and diseases. *BioFactors* **38**, 329–337
 18. Means, C. K., and Brown, J. H. (2009) Sphingosine-1-phosphate receptor signalling in the heart. *Cardiovasc. Res.* **82**, 193–200
 19. Fyrst, H., and Saba, J. D. (2010) An update on sphingosine-1-phosphate and other sphingolipid mediators. *Nat. Chem. Biol.* **6**, 489–497
 20. Ryu, Y., Takuwa, N., Sugimoto, N., Sakurada, S., Usui, S., Okamoto, H., Matsui, O., and Takuwa, Y. (2002) Sphingosine-1-phosphate, a platelet-derived lysophospholipid mediator, negatively regulates cellular Rac activity and cell migration in vascular smooth muscle cells. *Circ. Res.* **90**, 325–332
 21. Garcia, J. G., Liu, F., Verin, A. D., Birukova, A., Dechert, M. A., Gerthoffer, W. T., Bamberg, J. R., and English, D. (2001) Sphingosine 1-phosphate promotes endothelial cell barrier integrity by Edg-dependent cytoskeletal rearrangement. *J. Clin. Invest.* **108**, 689–701
 22. Lee, M.-J., Thangada, S., Claffey, K. P., Ancellin, N., Liu, C. H., Kluk, M., Volpi, M., Sha'afi, R. I., and Hla, T. (1999) Vascular endothelial cell adherens junction assembly and morphogenesis induced by sphingosine-1-phosphate. *Cell* **99**, 301–312
 23. Lee, J.-F., Gordon, S., Estrada, R., Wang, L., Siow, D. L., Wattenberg, B. W., Lominadze, D., and Lee, M.-J. (2009) Balance of S1P₁ and S1P₂ signaling regulates peripheral microvascular permeability in rat cremaster muscle vasculature. *Am. J. Physiol. Heart Circ. Physiol.* **296**, H33–H42
 24. Wang, F., Van Brocklyn, J. R., Hobson, J. P., Movafagh, S., Zukowska-Grojec, Z., Milstien, S., and Spiegel, S. (1999) Sphingosine 1-phosphate stimulates cell migration through a G_i-coupled cell surface receptor. *J. Biol. Chem.* **274**, 35343–35350
 25. Liu, U., Wada, R., Yamashita, T., Mi, Y., Deng, C.-X., Hobson, J. P., Rosenfeldt, H. M., Nava, V. E., Chae, S.-S., Lee, M.-J., Liu, C. H., Hla, T., Spiegel, S., and Proia, R. L. (2000) Edg-1, the G protein-coupled receptor for sphingosine-1-phosphate, is essential for vascular maturation. *J. Clin. Invest.* **106**, 951–961
 26. Jung, B., Obinata, H., Galvani, S., Mendelson, K., Ding, B.-S., Skoura, A., Kinzel, B., Brinkmann, V., Rafii, S., Evans, T., and Hla, T. (2012) Flow-regulated endothelial S1P receptor-1 signaling sustains vascular development. *Dev. Cell* **23**, 600–610
 27. Gaengel, K., Niaudet, C., Hagikura, K., Lavina, B., Muhl, L., Hofmann, J. J., Ebarasi, L., Nyström, S., Rymo, S., Chen, L. L., Pang, M., Jin, Y., Raschperger, E., Roswall, P., Schulte, D., Benedito, R., Larsson, J., Hellström, M., Fuxe, J., Uhlén, P., Adams, R., Jakobsson, L., Majumdar, A., Vestweber, D., Uv, A., and Betsholtz, C. (2012) The sphingosine-1-phosphate receptor S1PR1 restricts sprouting angiogenesis by regulating the interplay between VE-Cadherin and VEGFR2. *Dev. Cell* **23**, 587–599
 28. Ridley, A. J. (2011) Life at the leading edge. *Cell* **145**, 1012–1022
 29. Yamada, S., and Nelson, W. J. (2007) Localized zones of Rho and Rac activities drive initiation and expansion of epithelial cell-cell adhesion. *J. Cell Biol.* **178**, 517–527
 30. Heasman, S. J., and Ridley, A. J. (2008) Mammalian Rho GTPases. New insights into their functions from *in vivo* studies. *Nat. Rev. Mol. Cell Biol.* **9**, 690–701
 31. Mitra, S. K., Hanson, D. A., and Schlaepfer, D. D. (2005) Focal adhesion kinase. In command and control of cell motility. *Nat. Rev. Mol. Cell Biol.* **6**, 56–68
 32. Beningo, K. A., Hamao, K., Dembo, M., Wang, Y.-L., and Hosoya, H. (2006) Traction forces of fibroblasts are regulated by the Rho-dependent kinase but not by the myosin light chain kinase. *Arch. Biochem. Biophys.* **456**, 224–231
 33. Dobrowolski, R., and De Robertis, E. M. (2012) Endocytic control of growth factor signalling. Multivesicular bodies as signalling organelles. *Nat. Rev. Mol. Cell Biol.* **13**, 53–60
 34. Palamidessi, A., Frittoli, E., Garré, M., Faretta, M., Mione, M., Testa, I., Diaspro, A., Lanzetti, L., Scita, G., and Di Fiore, P. P. (2008) Endocytic trafficking of Rac is required for the spatial restriction of signaling in cell migration. *Cell* **134**, 135–147
 35. Zoncu, R., Perera, R. M., Balkin, D. M., Pirruccello, M., Toomre, D., and De Camilli, P. (2009) A phosphoinositide switch controls the maturation and signaling properties of APPL endosomes. *Cell* **136**, 1110–1121
 36. Okamoto, H., Takuwa, N., Yokomizo, T., Sugimoto, N., Sakurada, S., Shigematsu, H., and Takuwa, Y. (2000) Inhibitory regulation of Rac activation, membrane ruffling, and cell migration by the G protein-coupled sphingosine-1-phosphate receptor EDG5 but not EDG1 or EDG3. *Mol. Cell Biol.* **20**, 9247–9261
 37. Sugimoto, N., Takuwa, N., Okamoto, H., Sakurada, S., and Takuwa, Y. (2003) Inhibitory and stimulatory regulation of Rac and cell motility by the G_{12/13}-Rho and G_i pathways integrated downstream of a single G protein-coupled sphingosine-1-phosphate receptor isoform. *Mol. Cell Biol.* **23**, 1534–1545
 38. Sakurada, S., Okamoto, H., Takuwa, N., Sugimoto, N., and Takuwa, Y. (2001) Rho activation in excitatory agonist-stimulated vascular smooth muscle. *Am. J. Physiol. Cell Physiol.* **281**, C571–C578
 39. Eccles, S. A., Court, W., Patterson, L., and Sanderson, S. (2009) *In vitro* assays for endothelial cell functions related to angiogenesis. Proliferation, motility, tubular differentiation, and proteolysis. *Methods Mol. Biol.* **467**, 159–181
 40. Usui, S., Sugimoto, N., Takuwa, N., Sakagami, S., Takata, S., Kaneko, S., and Takuwa, Y. (2004) Blood lipid mediator sphingosine 1-phosphate potently stimulates platelet-derived growth factor-A and -B chain expression through S1P1-Gi-Ras-MAPK-dependent induction of Krüppel-like factor 5. *J. Biol. Chem.* **279**, 12300–12311
 41. Du, W., Takuwa, N., Yoshioka, K., Okamoto, Y., Gonda, K., Sugihara, K., Fukamizu, A., Asano, M., and Takuwa, Y. (2010) S1P2, the G protein-coupled receptor for sphingosine-1-phosphate, negatively regulates tumor angiogenesis and tumor growth *in vivo* in mice. *Cancer Res.* **70**, 772–781
 42. Itoh, R. E., Kurokawa, K., Ohba, Y., Yoshizaki, H., Mochizuki, N., and Matsuda, M. (2002) Activation of Rac and Cdc42 video imaged by fluorescent resonance energy transfer-based single-molecule probes in the membrane of living cells. *Mol. Cell Biol.* **22**, 6582–6591
 43. Sasaki, T., Irie-Sasaki, J., Jones, R. G., Oliveira-dos-Santos, A. J., Stanford, W. L., Bolon, B., Wakeham, A., Itie, A., Bouchard, D., Kozieradzki, I., Joza, N., Mak, T. W., Ohashi, P. S., Suzuki, A., and Penninger, J. M. (2000) Function of PI3K γ in thymocyte development, T cell activation, and neutrophil migration. *Science* **287**, 1040–1046
 44. Sasaki, J., Sasaki, T., Yamazaki, M., Matsuoka, K., Taya, C., Shitara, H., Takasuga, S., Nishio, M., Mizuno, K., Wada, T., Miyazaki, H., Watanabe, H., Iizuka, R., Kubo, S., Murata, S., Chiba, T., Maehama, T., Hamada, K., Kishimoto, H., Frohman, M. A., Tanaka, K., Penninger, J. M., Yonekawa, H., Suzuki, A., and Kanaho, Y. (2005) Regulation of anaphylactic responses by phosphatidylinositol phosphate kinase type I α . *J. Exp. Med.* **201**, 859–870
 45. Igarashi, J., and Michel, T. (2001) Sphingosine 1-phosphate and isoform-specific activation of phosphoinositide 3-kinase β . *J. Biol. Chem.* **276**, 36281–36288
 46. Cain, R. J., and Ridley, A. J. (2009) Phosphoinositide 3-kinases in cell migration. *Biol. Cell* **101**, 13–29
 47. Xu, K., Sacharidou, A., Fu, S., Chong, D. C., Skaug, B., Chen, Z. J., Davis, G. E., and Cleaver, O. (2011) Blood vessel tubulogenesis requires Rasip1

- regulation of GTPase signaling. *Dev. Cell* **20**, 526–539
48. Broussard, J. A., Lin, W. H., Majumdar, D., Anderson, B., Eason, B., Brown, C. M., and Webb, D. J. (2012) The endosomal adaptor protein APPL1 impairs the turnover of leading edge adhesions to regulate cell migration. *Mol. Biol. Cell* **23**, 1486–1499
 49. Zaidel-Bar, R., Milo, R., Kam, Z., and Geiger, B. (2007) A paxillin tyrosine phosphorylation switch regulates the assembly and form of cell-matrix adhesions. *J. Cell Sci.* **120**, 137–148
 50. Hall, A., and Nobes, C. D. (2000) Rho GTPases. Molecular switches that control the organization and dynamics of the actin cytoskeleton. *Philos. Trans. R. Soc. Lond. B Biol. Sci.* **355**, 965–970
 51. Higuchi M., Masuyama, N., Fukui, Y., Suzuki, A., and Gotoh, Y. (2001) Akt mediates Rac/Cdc42-regulated cell motility in growth factor-stimulated cells and in invasive PTEN knockout cells. *Curr. Biol.* **11**, 1958–1962
 52. Lee, M. J., Thangada, S., Paik, J. H., Sapkota, G. P., Ancellin, N., Chae, S. S., Wu, M., Morales-Ruiz, M., Sessa, W. C., Alessi, D. R., and Hla, T. (2001) Akt-mediated phosphorylation of the G protein-coupled receptor EDG-1 is required for endothelial cell chemotaxis. *Mol. Cell* **8**, 693–704
 53. Macia, E., Ehrlich, M., Massol, R., Boucrot, E., Brunner, C., and Kirchhausen, T. (2006) Dynasore, a cell-permeable inhibitor of dynamin. *Dev. Cell* **10**, 839–850
 54. Kutateladze, T. G. (2010) Translation of the phosphoinositide code by PI effectors. *Nat. Chem. Biol.* **6**, 507–513
 55. Oo, M. L., Chang, S.-H., Thangada, S., Wu, M.-T., Rezaul, K., Blaho, V., Hwang, S.-I., Han, D. K., and Hla, T. (2011) Engagement of S1P₁-degradative mechanisms leads to vascular leak in mice, *The Journal of Clinical Investigation* **121**, 2290–2300
 56. Sorkin, A., and von Zastrow, M. (2009) Endocytosis and signalling. Inter-twining molecular networks. *Nat. Rev. Mol. Cell Biol.* **10**, 609–622
 57. Welch, H. C., Coadwell, W. J., Ellson, C. D., Ferguson, G. J., Andrews, S. R., Erdjument-Bromage, H., Tempst, P., Hawkins, P. T., and Stephens, L. R. (2002) P-Rex1, a PtdIns(3,4,5)P₃- and G₁₃-regulated guanine-nucleotide exchange factor for Rac. *Cell* **108**, 809–821
 58. Wertheimer, E., Gutierrez-Uzquiza, A., Rosembly, C., Lopez-Haber, C., Sosa, M. S., and Kazanietz, M. G. (2012) Rac signaling in breast cancer. A tale of GEFs and GAPs. *Cell Signal.* **24**, 353–362
 59. Windh, R. T., Lee, M.-J., Hla, T., An, S., Barr, A. J., and Manning, D. R. (1999) Differential coupling of the sphingosine 1-phosphate receptors Edg-1, Edg-3, and H218/Edg-5 to the G_i, G_q, and G₁₂ families of heterotrimeric G proteins. *J. Biol. Chem.* **274**, 27351–27358
 60. Mullershausen, F., Zecri, F., Cetin, C., Billich, A., Guerini, D., and Seuwen, K. (2009) Persistent signaling induced by FTY720-phosphate is mediated by internalized S1P₁ receptors. *Nat. Chem. Biol.* **5**, 428–434
 61. Maffucci, T., Cooke, F. T., Foster, F. M., Traer, C. J., Fry, M. J., and Falasca, M. (2005) Class II phosphoinositide 3-kinase defines a novel signaling pathway in cell migration. *J. Cell Biol.* **169**, 789–799
 62. Domin, J., Harper, L., Aubyn, D., Wheeler, M., Florey, O., Haskard, D., Yuan, M., and Zicha, D. (2005) The class II phosphoinositide 3-kinase PI3K-C2 β regulates cell migration by a PtdIns3P-dependent mechanism. *J. Cell Physiol.* **205**, 452–462
 63. Katso, R. M., Pardo, O. E., Palamidessi, A., Franz, C. M., Marinov, M., De Laurentis, A., Downward, J., Scita, G., Ridley, A. J., Waterfield, M. D., and Arcaro, A. (2006) Phosphoinositide 3-kinase C2 β regulates cytoskeletal organization and cell migration via Rac-dependent mechanisms. *Mol. Biol. Cell* **17**, 3729–3744
 64. Gould, G. W., and Lippincott-Schwartz, J. (2009) New roles for endosomes. From vesicular carriers to multi-purpose platforms. *Nat. Rev. Mol. Cell Biol.* **10**, 287–292